Chitosan-Paracetamol Nanostructure Self-Assembling Matrices as Drug Delivery Systems

ANA GARLEA[1]*, ALINA MANOLE[1], MARCEL IONEL POPA[2], VIOREL MELNIG[1]

[1] "Al. I. Cuza" University, Faculty of Physics, 11A Carol I Blvd., 700506, Iasi, Romania

[2] "Gh. Asachi" University, Faculty of Chemistry, 71A D. Mangeron Blvd., 700050, Iasi, Romania

The amphiphilic polymers can form associated structures in aqueous solution by mutual interaction and/or interaction with other components such as surfactants and active colloidal molecules. In this paper, results regarding nanolevel associative behaviour of chitosan based systems with surfactant and paracetamol are presented. The viscosity measurements of the solutions prepared were made with a view to take into consideration viscosity as an associative parameter. The thin films topography obtained by spin-coating was analyzed by Atomic Force Microscopy (AFM). The nanostructured matrices were investigated by Scanning Electronic Microscopy (SEM), X-Ray Diffraction (XRD) and by Fourier Transform InfraRed (FTIR) Spectroscopy. From FTIR and X-Ray investigations it can be concluded that, at nano - level, in the chitosan matrix, crystalline surfactant and paracetamol domains like nanocapsules are localized. By visual analysis of the AFM and SEM images it can be observed that the nanocapsules are orderly structured in horizontal layers and present a vertical gradient, the paracetamol nanocapsules formed having dimensions in the range of 21 – 170 nm. The chitosan-paracetamol nanostructured matrices obtained by the phase inversion method stand as a remarkable candidate to be used to control release of this drug.

Keywords: chitosan, paracetamol, cationic surfactant, structural analysis.

Chitosan is an inert, hydrophilic, biocompatible and biodegradable polymer [1]. The unique structural feature of chitosan is the high content of primary amines, and these amines confer important functional properties to chitosan like the polyelectrolyte character depending on pH. Thus, at low pH chitosan is water-soluble, while at high pH it becomes insoluble. The soluble-insoluble transition occurs at *p*H of 6 - 6.5, this *p*H range being of high interest for biological applications [2]. Chitosan amines physically interact with different ionic surfactants, allowing to functionalize the chitosan or to cross-link the chitosan backbone to confer elasticity. Chitosan can easily form films or membranes under mild acidic aqueous conditions, and their quality is affected by the differences in chitosan properties, solvents used, methods of preparation, and types and amount of surfactants used [3].

Paracetamol has been used as an analgesic and antipyretic for many years, with toxicity first noted in the 1960s. Since then the incidence of poisoning has increased, and paracetamol is now the most common drug in self-poisoning, with a high rate of morbidity and mortality. A healthy adult who takes more than 10 to 12 grams in one dose or more than 7.5 g a day for a longer period, risks liver damage [4].

The objectives of this study are the preparation and characterization of freestanding cross-linked chitosan films and membranes prepared by the dry phase inversion method from solutions of chitosan in acetic acid, in the presence of a moderate amount of surfactant. Also, the paracetamol was entrapped in this matrix aiming its application as controlled drug delivery systems.

Experimental Part

Materials and methods

The paracetamol, with a molecular weight of 151.17 g/mol, was acquired from Sigma Aldrich. The chitosan was provided by Vanson Chemicals Redmond WA, USA. The N-deacetylation degree was 79.7%, the average molecular weight was M_w = 310,000 g/mol and the polydispersity index was 3.26. Two types of surfactants were used: a cationic one, cetyltrimethylammonium bromide ($C_{19}H_{42}BrN$) (CTAB) purchased from Chemapol and an anionic one, sodium dodecyl sulfate ($C_{12}H_{25}NaO_4S$) (SDS) purchased from Sigma Aldrich.

Chitosan solutions (2 and 3%*w*/*w* biopolymer concentration in 1% *v*/*v* acetic acid aqueous solution) with different surfactant concentrations (2, 4, 6, 8 and 10 m*m*; where *m* represents the molal concentration, the number of moles of solute per 1000 g of solvent: $m = N_d(1000 / G_s)$; N_d – the solute amount expressed in moles and G_s - the solvent amount expressed in grams) were prepared.

The mixtures were stirred at room temperature for 24 h, and the solutions were degassed by centrifugation at 4000 rpm for 30 min.

Two matrices of 2 and 3% w/w chitosan solutions were prepared by mixing them with different anionic/cationic surfactant concentrations (2, 4, 6, 8 and 10 m*m*).

The 2 and 3% *w*/*w* chitosan membranes with 6 m*m* cationic surfactant (CTAB) and different concentrations of paracetamol (1, 2, 3, 5, 7 and 10 m*m*), were prepared by dry phase inversion [5]: the solutions were poured into Teflon molds and left to evaporate in a thermostat chamber at 50°C for 24 h.

The films were obtained by depositing on supports by spin-coating method using a WS-400B-6NPP/LITE spin-coater.

Characterization methods

The solutions were subjected to rotational tests at controlled shear rate, at 25°C using a Haake Viscotester 7 plus.

* email: anagarlea@yahoo.com

The film topographies were analyzed by Atomic Force Microscopy (AFM) using a Solver Pro 7M apparatus. The analysis was taken in tapping mode.

The membranes morphology was studied by Scanning Electron Microscopy (SEM) on a VEGA TESCAN apparatus. The nanocapsule size was determined by comparison with a standard scale of SEM micrographies using NIS Elements Basic Research imaging software. To determine their distribution it was used the same statistical program.

Structural analysis was performed by X-Ray diffraction (XRD) performed on a DRON-2 diffractometer, employing nickel-filtered Cu K_α radiation (1.54182 Å) at 25 kV operational voltage and by Fourier Transform InfraRred (FTIR) spectroscopy using a BOMEM MB-104 spectrometer, with 4 cm^{-1} resolution, in the range 4000-500 cm^{-1}.

Results and discussions

Rheological behaviour of the two solutions of chitosan 2 and 3% is specific for the two surfactants used and more evident with chitosan concentration increasing. Results of viscosity measurements for 3% chitosan solution for the two surfactants used are shown in figure 1.

The viscosity of the chitosan solutions in the presence of CTAB increases with the increase of CTAB concentration. For SDS – chitosan solution the viscosity reaches the maximum value for 10 m*m* and 4 m*m* SDS concentration.

From the behaviour of chitosan solution viscosity dependence as function of SDS concentration it can be observed that these solutions present a higher instability degree due to association/dissociation force ratio drastic modification with the SDS concentration, which entitles us to consider that the solutions do not present stability when the paracetamol is introduced in the system. More appropriate for our purpose are the chitosan-CTAB solutions. A second potent argument represents the low toxicity of the CTAB surfactant compared to SDS [6].

The obtained membranes containing CTAB are transparent and flexible, properties that are maintained in time, unlike the pure chitosan membrane and those with chitosan and drug which, the thicker they are the more rigid and breakable become, properties that are enhanced in time [7].

The FTIR spectra for 2% pure chitosan membrane and 2% chitosan membranes with 2, 6 and 10 m*m* CTAB are shown in figure 2; no major differences are obtained in the case of 3% chitosan membranes with CTAB. Chitosan spectrum exhibits characteristic absorption bands of amide I at 1650 cm^{-1} (C = O stretching), amide II at 1550 cm^{-1} (N – H in plane deformation coupled with C – N stretching), amide III (C – N stretching coupled with NH in plane deformation) and CH_2 wagging coupled with OH in plane deformation at 1317 cm^{-1}. In the functional group region the broad peak observed at 3450 – 3200 cm^{-1} is the result of the different vibrations, specifically the hydrogen-bonded OH stretching at 3429 cm^{-1}, the NH_2 asymmetric stretching at 3360 cm^{-1} and the NH stretching in interchain NH ···O = C bonding at 3270 cm^{-1}. The other peaks at 2910 cm^{-1} and 1397 cm^{-1} were assigned to CH stretching and CH_3 symmetric deformation, respectively. Anti-symmetric stretching of C – O – C gives a narrow band at 1157 cm^{-1}.

The skeletal vibrations involving the C – O stretching at 1070 and 1020 cm^{-1} are characteristic bands of the chitosan saccharide structure [7 - 9]. The absence of sharp absorption peak around 3500 cm^{-1} indicated that there are no free OH groups.

Comparing the spectrum of 2% pure chitosan membrane with those of chitosan membranes with CTAB, from figure 2, despite the fact that both molecules (chitosan and CTAB) present cationic character, it can be observed that interactions occur, and this is evidenced by the groups absorption bands modification.

While in the fingerprint region the absorption bands intensities are proportionally attenuated with CTAB concentration increasing, in respect of position and profile of absorption bands, the functional group region is drastically affected by the presence of CTAB at whatever concentration; peaks being observed beyond 3500 cm^{-1}. The bands within 3500 – 3000 cm^{-1} shifted to higher frequencies indicate an increase in the ordered structure [10]. The region 1500 – 1200 cm^{-1} is related to the local symmetry. To summarize, it was expected a high degree of order at the molecular assembly level in detriment of molecular symmetry.

Figure 3 shows the X-ray diffractograms of chitosan membranes with 2% concentration, in the presence of CTAB (similar results were obtained for 3% chitosan membranes). The X-ray diffractogram of pure chitosan shows an almost amorphous structure while, as expected, the membranes with CTAB show an apparent increase in crystallinity with the increase of CTAB concentration. The fact that the intensity of diffraction peaks increases with the increase of CTAB concentration, without any modification of the position of those peaks in diffractogram, shows that these diffractograms are the result of interference patterns composition from the two structures, the chitosan matrix and CTAB clusters.

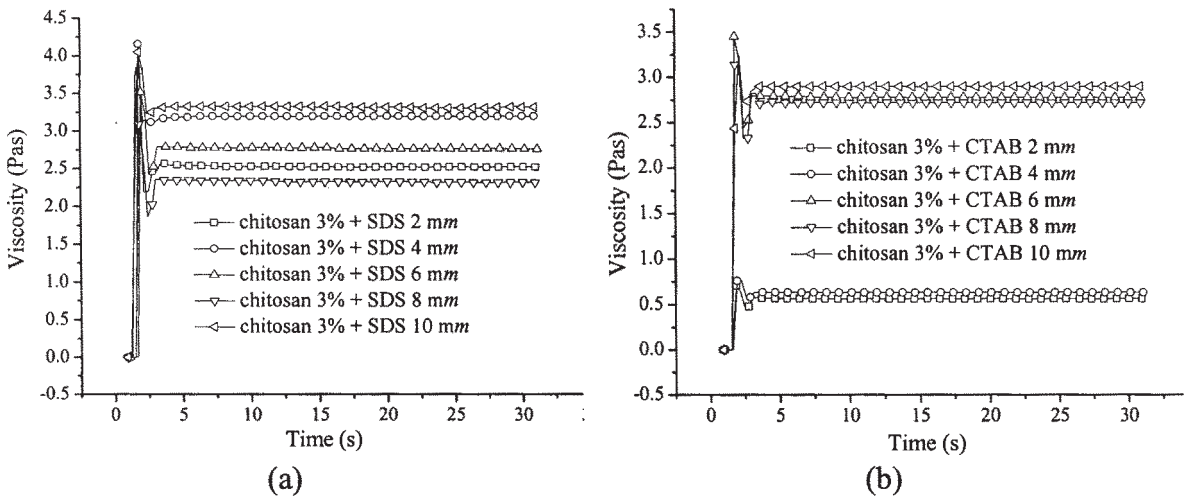

Fig. 1. Viscosity dependence on the surfactant type and concentration: (a) SDS and (b) CTAB, for 3% chitosan concentration solution

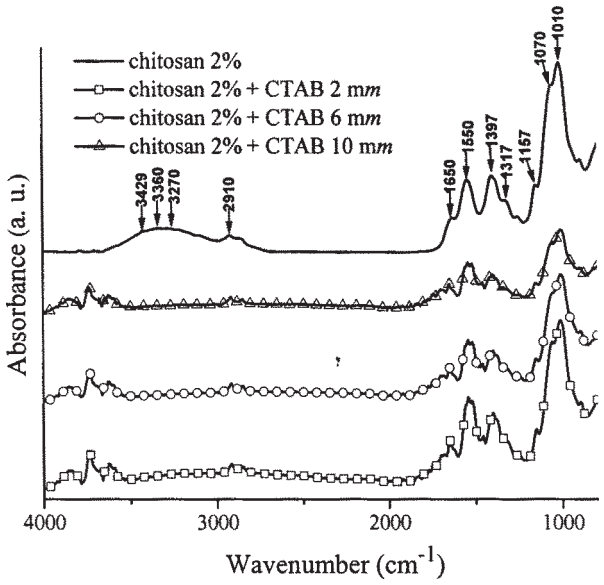

Fig. 2. FTIR spectra for 2% pure chitosan membrane and chitosan membranes in the presence of different concentrations of CTAB

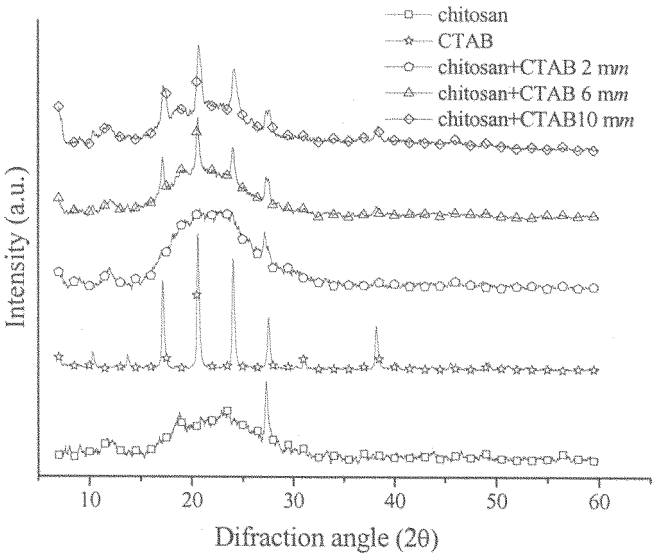

Fig. 3. X-Ray diffractograms for 2% chitosan membranes in the presence of different CTAB concentrations

The SEM micrographies (fig. 4) for chitosan membranes with 2 and 3% concentration, in the presence of different CTAB amounts attest these presumptions; the membranes are dense and have a uniform distribution of the CTAB nanocrystals.

For a better understanding of the molecular assembled processes (as it was realized in the previous paper [11]) AFM topographies of different combinations of films constituents have been performed. In figure 5 are presented the AFM images of pure 2% chitosan, 2% chitosan with 2 m*m* paracetamol and 2% chitosan with 6 m*m* CTAB. It can be observed that the chitosan and paracetamol-chitosan system films are homogeneous while the CTAB-chitosan system films have a heterogeneous morphology with a good regularity at the mesophasic level.

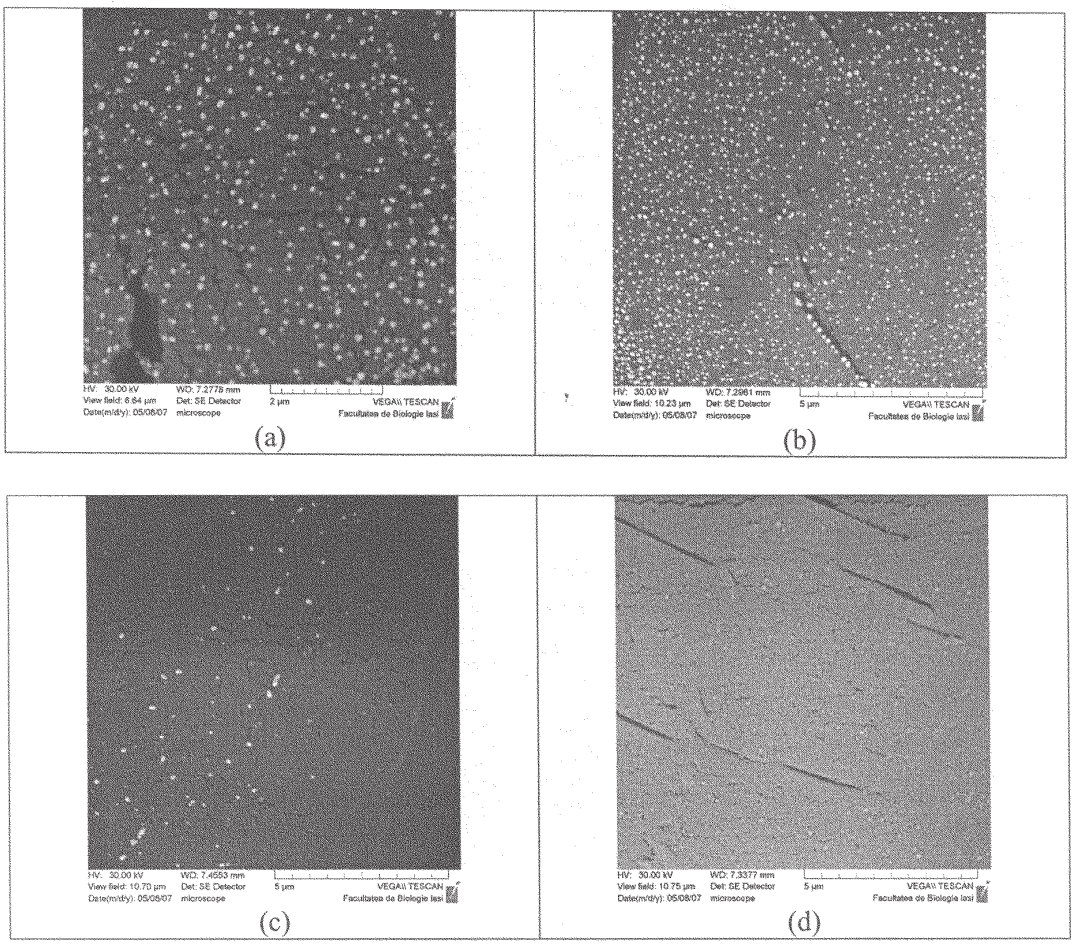

Fig. 4. SEM micrographies of the air-facing surfaces for 2% chitosan membranes with 6 m*m* CTAB (a) and 10 m*m* CTAB (b), and 3% chitosan membranes with 6 m*m* CTAB (c) and 10 m*m* CTAB (d)

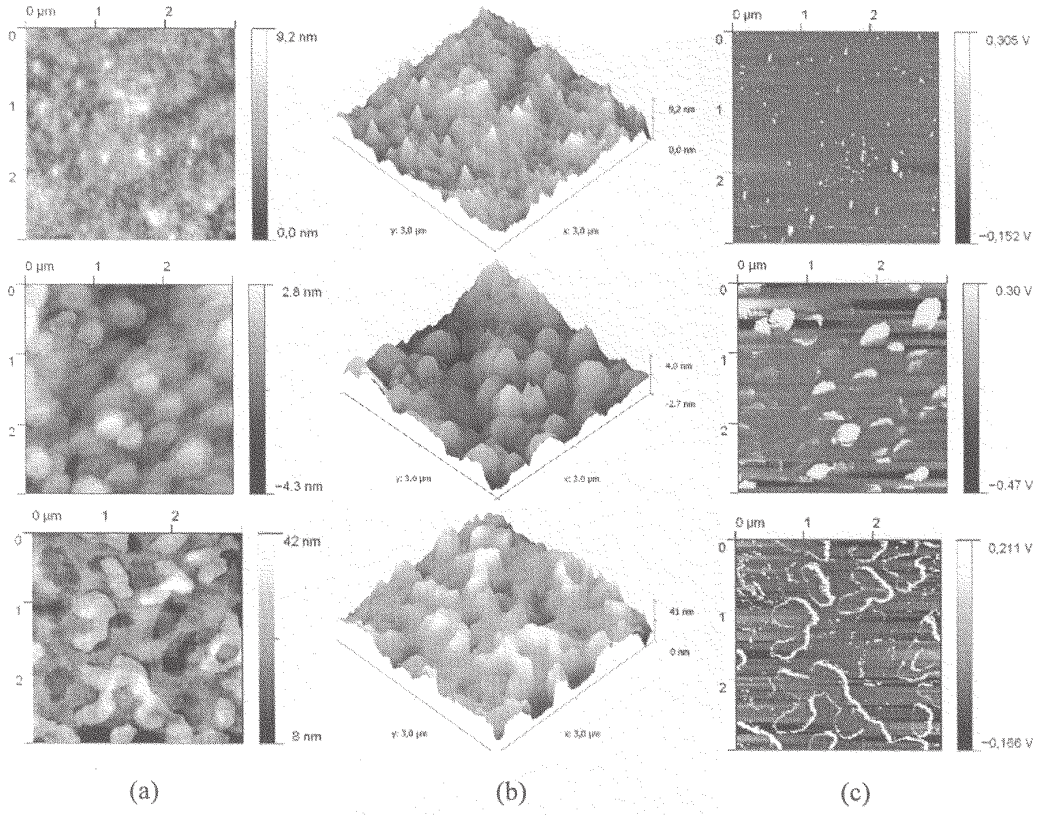

Fig. 5. The 2D (a) and 3D (b) topographies, and phase contrast (c) of 2% chitosan film (top), 2% chitosan with 2 m*m* paracetamol film (middle), 2% chitosan with 6 m*m* CTAB film (bottom); the scale of square area is 3 x 3µm^2.

Previous studies show that, in the absence of cross-linking molecules, the chitosan membranes obtained are rigid and brittle. Moreover, a relatively large drying time determines a dense membrane formation in which the internal tensions increase with the membrane thickness [7, 12]. In the case of surfactant addition, the fact that chitosan membranes are flexible as well as the results obtained from FTIR, XRD and AFM analysis entitle us to affirm that the internal tensions, arising from solidification of chitosan membrane, become locally distributed at the interface with CTAB nanometer domains. It is possible that the repulsion interactions occurring between the two types of molecules (chitosan and CTAB), due to their cationic behaviour in aqueous solution, to reduce the internal

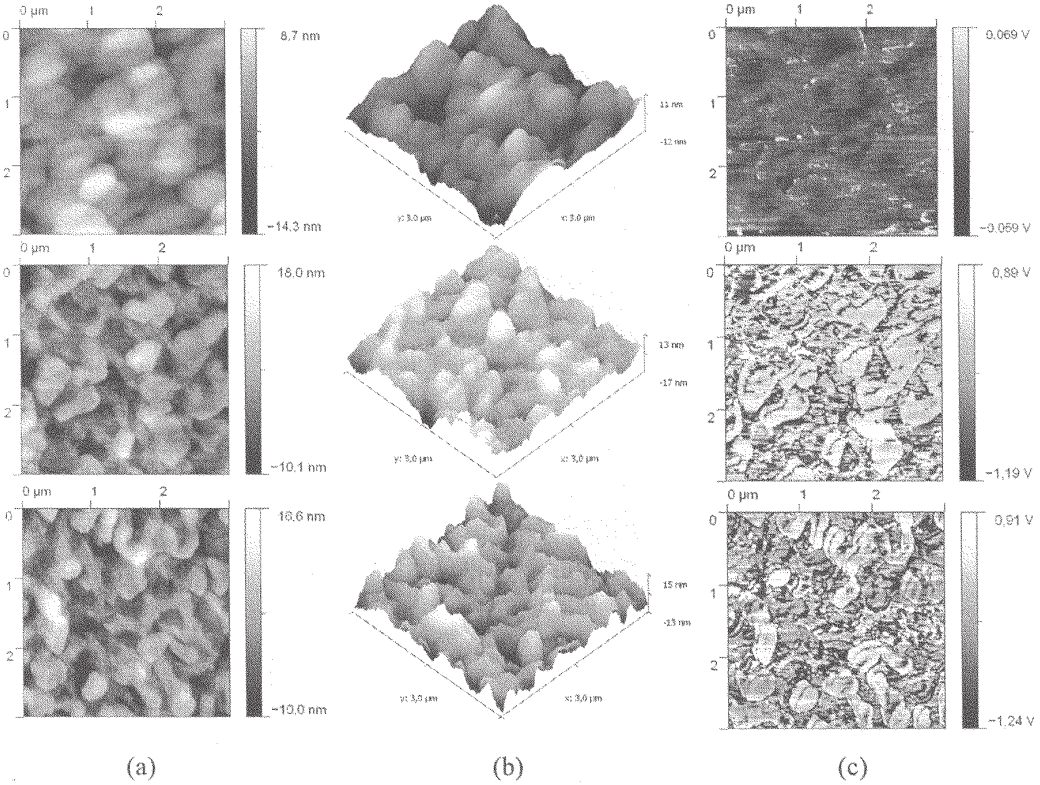

Fig. 6. 2D (a) and 3D (b) topographies, and phase contrast (c) of 2% chitosan and 6 m*m* CTAB films in combination with paracetamol: 5 m*m* (top), 7 m*m* (middle), 10 m*m* (bottom); the scale of square area is 3 x 3 µm^2.

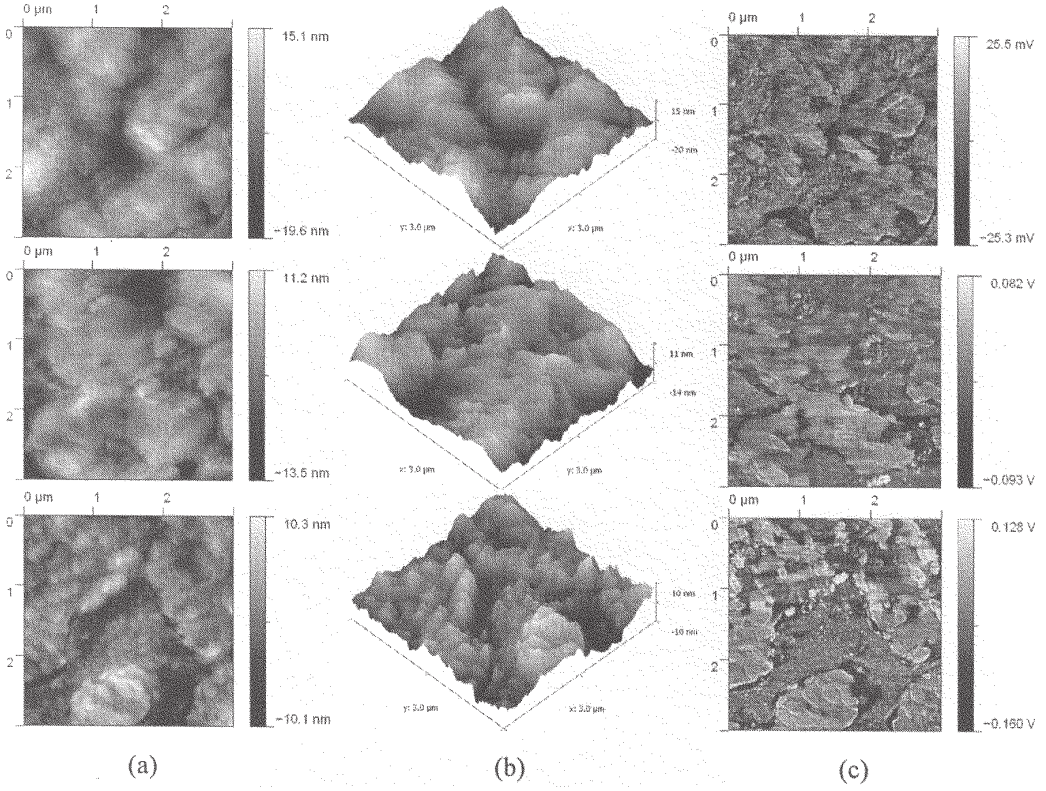

Fig. 7. 2D (a) and 3D (b) topographies, and phase contrast (c) of 3% chitosan and 6 m*m* CTAB films in combination with paracetamol: 5 m*m* (top), 7 m*m* (middle), 10 m*m* (bottom); the scale of square area is 3x3 µm^2

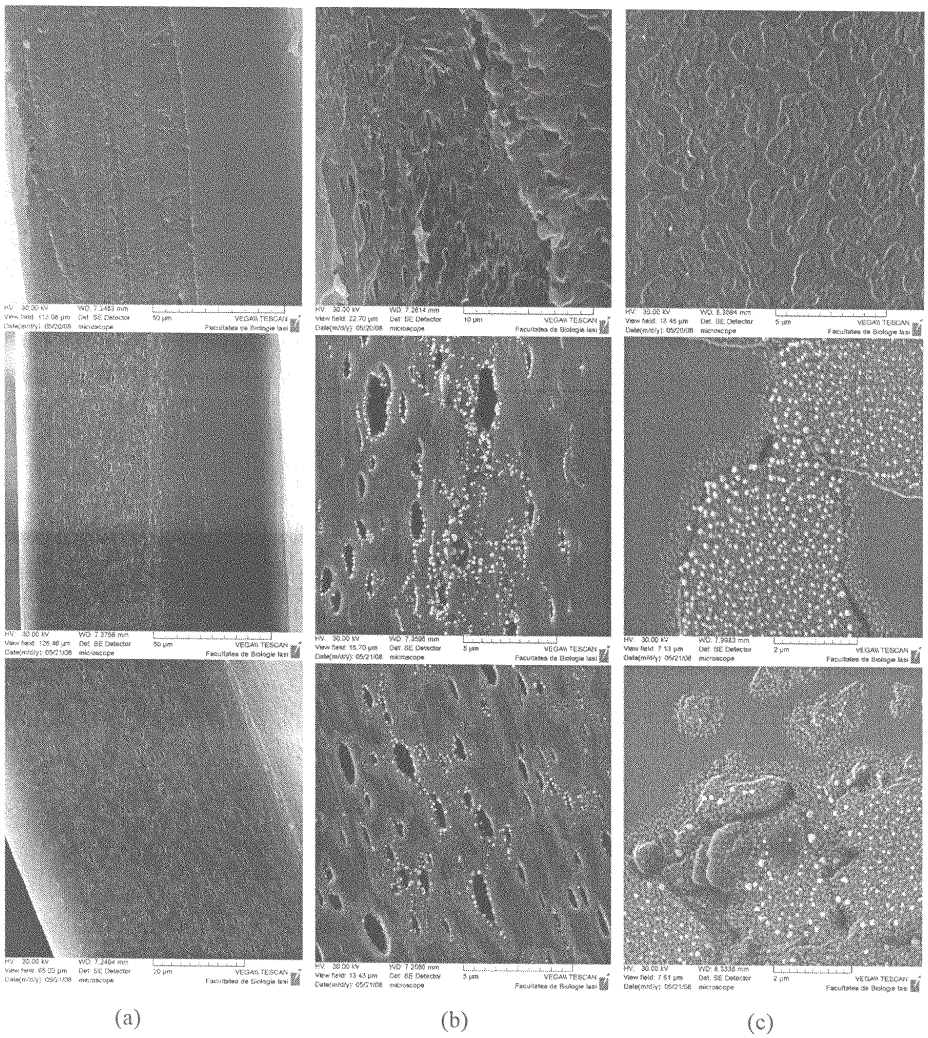

Fig. 8. SEM micrographies of transversal section (a), transversal section details (b) and air-facing surface (c) of 2% chitosan and 6 m*m* CTAB membranes in combination with paracetamol: 5 m*m* (top), 7 m*m* (middle), 10 m*m* (bottom)

tensions. In addition, the fact that the solidification process of the membrane, held in constant temperature, is completed with a mixture of two solid phases in equilibrium (there is no phase separation), we can consider that the system in liquid phase passes through several quasiequilibrium states until an appreciable amount of

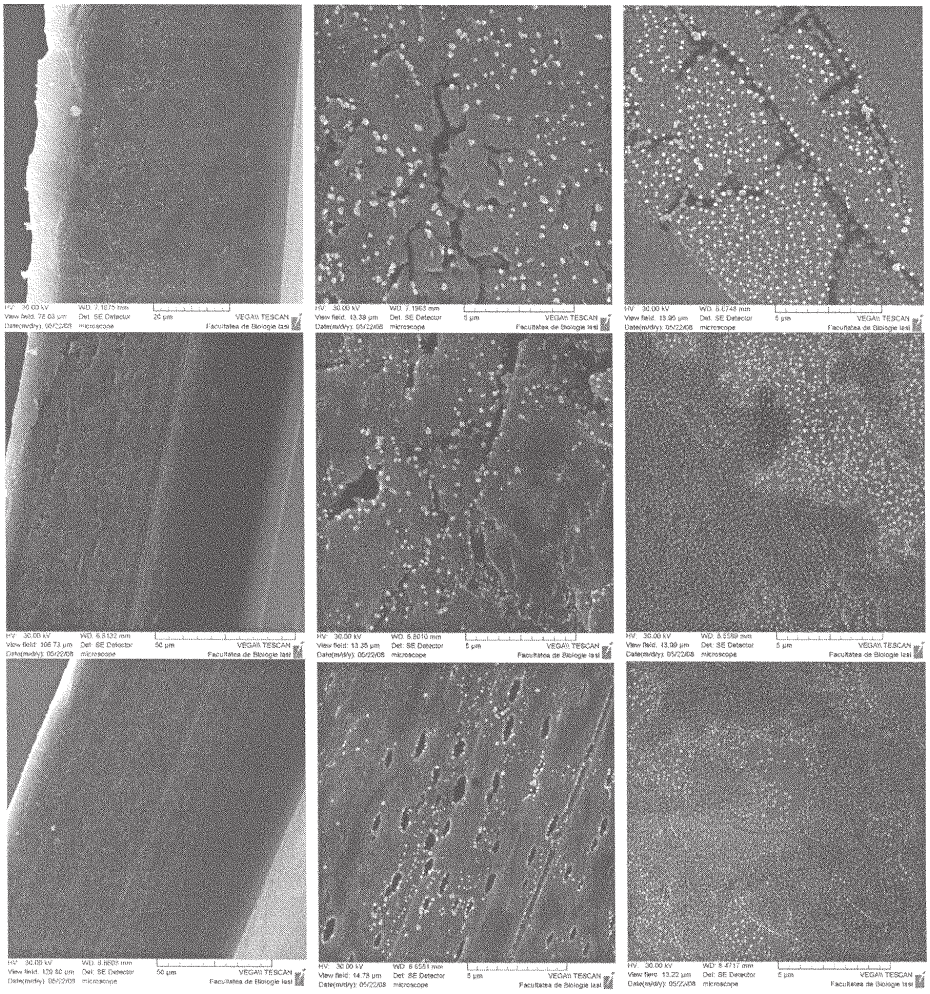

(a) (b) (c)

Fig. 9. SEM micrographies of transversal section (a), transversal section details (b) and air-facing surface (c) of 3% chitosan and 6 m*m* CTAB membranes in combination with paracetamol: 5 m*m* (top), 7 m*m* (middle), 10 m*m* (bottom)

solvent (water) is lost and the system becomes a solid membrane. It is important to discuss at least two antagonistic processes competing to achieve system stability: the migration process due to mutual repulsions between the two types of cationic molecules and the process due to CTAB molecules diffusion. The measure of kinetic forces associated with those highly determines the nanocapsules size and their uniform distribution in the horizontal planes. From the structural FTIR analysis shows that there is interaction between the two types of molecules. From the structural point of view, FTIR analysis shows that there are interactions between the two types of molecules. Any disturbance of a molecule from the *in vacuum* state alters the symmetry of the isolated molecule. On the other hand, the interactions between these two types of molecules lead to a local order at nanometer level of CTAB domains without a major influence on crystalline degree of chitosan matrix.

The results obtained for viscosity and SEM analysis make us to consider an optimum domain for CTAB concentration in the range 6 - 10 m*m*. Practically, a minimum concentration of 6 m*m* CTAB was chosen to reduce to a minimum the effects due to this surfactant, although it is considered as having a low toxicity [6].

Based on these arguments, we used systems of 6 m*m* CTAB with 2% and 3% chitosan as precursors for nanostructured matrix containing different concentrations of paracetamol. In figures 6 and 7 are presented the AFM images of these films.

Net structures of those types that can be seen at the bottom of figure 5 for CTAB do not appear and the fact that these structures have a geometrical form approximately of the same type and increase in ponderosity with the increase of the paracetamol concentration entitles us to believe that they contain a paracetamol – CTAB mixture (they are capsules).

Figures 6 and 7 indicate that better defined structures are formed for 2% chitosan concentration than for 3% chitosan concentration and in the case of 7 and 10 m*m* paracetamol concentration.

To support the previous statements, SEM micrographies (figs. 8 and 9) were recorded for 2 and 3% chitosan and 6 m*m* CTAB membranes in the same paracetamol concentration range as for films.

The SEM images demonstrate an ordering of the paracetamol–CTAB nanocapsules in horizontal planes of chitosan matrix, which means that these nanocapsules will release in a controlled manner the active substance (paracetamol) as the chitosan matrix is subject of the erosion-swelling process.

The nanocapsules size analysis from SEM micrography of the surface for the 2% chitosan with 6 m*m* CTAB and 7 m*m* paracetamol representative sample (fig. 8 - middle), shows that the nanocapsules formed have dimensions in the range 21 - 170 nm with a maximum distribution at 40 nm. In figure 10 are presented details of statistical analysis.

Both chitosan and paracetamol concentration increase leads to diminishing the degree of order in the system,

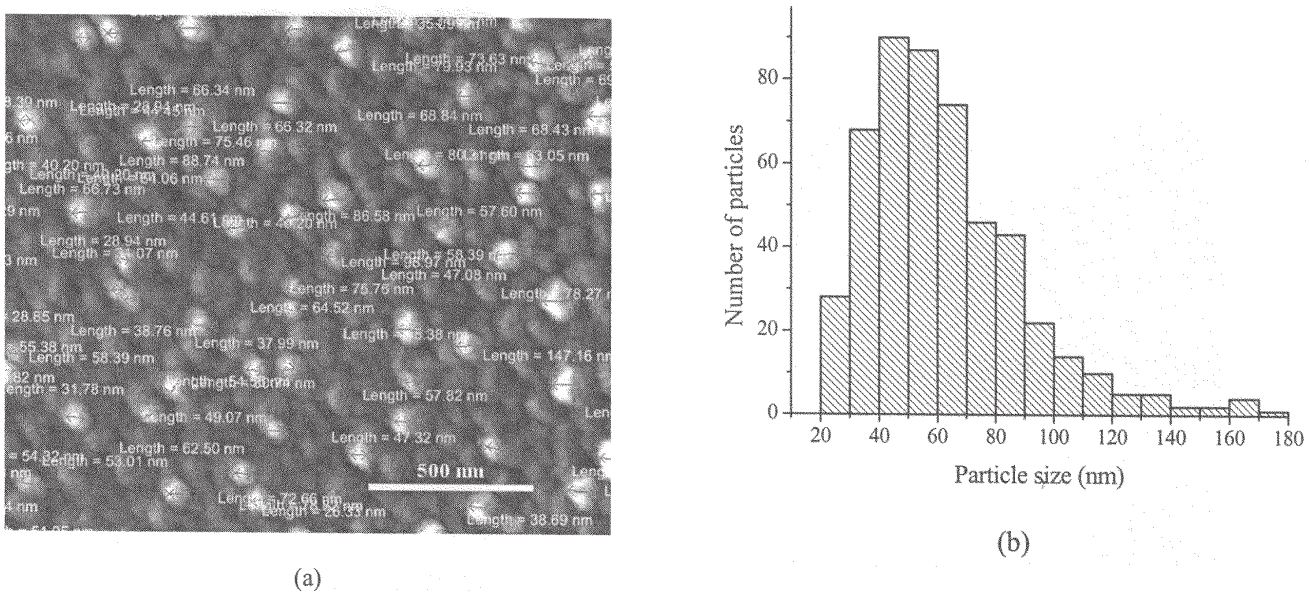

Fig. 10. a) SEM micrography detail of the surface from figure 8 – middle containing measuring data by comparison with the standard scale of nanocapsules dimensions. b) Size histogram for this SEM micrography

determining the nanocapsules ponderosity to decrease, which is in a good concordance with the AFM images.

Conclusively, the best results are obtained for a concentration of 2% chitosan, 6 m*m* CTAB and 7-10 m*m* paracetamol. For a concentration higher than 10 m*m* paracetamol, the nanocapsules vanish.

Conclusions

Membranes with a high degree of order at the nanoscale level were obtained by dry phase inversion preparation from solutions of chitosan in acetic acid, in the presence of a moderate amount of surfactant.

The viscosity of the chitosan solutions depends on the type and concentration of the surfactant, the chitosan-CTAB solutions being more stable than the chitosan-SDS ones.

From the SEM, FTIR and X-Ray investigations of chitosan - CTAB membranes it can be observed that in the chitosan matrix crystalline CTAB domains are localized, due to at least two antagonistic processes competing to achieve system stability: the migration process due to mutual repulsions between the two types of cationic molecules and the process due to CTAB molecules diffusion.

The measure of kinetic forces associated with those processes highly determines the nanocapsules size and their uniform distribution in the horizontal planes. At higher levels of surfactant addition the crystals are more numerous but no significant differences in the dimension are observed. Thus, we consider that the optimum CTAB concentration for matrix nanostructuring is of 6 m*m*.

Analyzing the AFM topographies, it was observed that better defined structures are formed at 2% chitosan concentration, within 7 and 10 m*m* paracetamol concentration.

Nanocapsules size analysis from SEM image of the surface for the 2% chitosan with 6 m*m* CTAB and 7 m*m* paracetamol representative sample showed that the paracetamol nanocapsules formed have dimension in the range 21 - 170 nm with a maximum distribution at 40 nm.

The fact that the nanocapsules are orderly structured in planes, entitle us to affirm that as the chitosan is subjected to a swelling – erosion process, the paracetamol - CTAB capsules are dissolved and will release the active substance (paracetamol).

Acknowledgements

This study was financially supported by PN II Capacitati 195CPI/2008 and by PN II TD 17/2008.

References

1. LEE, K.Y., HA, W.H., Biomaterials, **16**, 1995, p. 1211
2. YI, H., WU, L.-Q., BENTLEY, W.E., GHODSSI, R., RUBLOFF, G.W., CULVER, J.N., PAYNE, G.F., Biomacromolecules, **6**, no. 6, 2005, p. 2881
3. NUNTHANID, J., PUTTIPIPATKHACHORN, S., YAMAMOTO, K., PEEK, G.E., Drug Dev. Ind. Pharm, **27**, 2001, p. 143
4. LARSON, A.M., POLSON, J., FONTANA, R.J., et al, Hepatology, **42,** no. 6, 2005, p. 1364
5. GARGANCIUC, D., BATRANESCU, GH., POPA, O., OLTEANU, M., Mat. Plast., **45**, no. 2, 2008, p. 167
6. ISOMAA, B., REUTER, J., DJUPSUND, B. M., Arch Toxicol **35**, 1976, p.91
7. BALAU, L., LISA, G., POPA, M.I., TURA, V., MELNIG, V., Central European Journal of Chemistry, **2**, no.4, 2004, p. 638
8. MONAL, W.A., PENICHE, C., Makromol. Chem., **9**, 1988, p. 693
9. ROBERTS, G. A. F., Chitin Chemistry, Macmillan, London, 1992
10. FOCHER, B., NAGGI, A., TORRI, G., COSANNI, A., TERBOJEVICH, M., Carbohydrate Polymers, **18**, 1992, p. 43
11. GARLEA, A., MELNIG, V., POPA, M. I., RUSU, G., Mat. Plast., **45**, no. 2, 2008, p. 193
12. MATSUYAMA, H., SHIRAISHI, H., KITAMURA, Y., Journal of Applied Polymer Science **73**, 1999, p. 2715

Manuscript received: 13.11.2008